

Simulation of Air-Supply Systems Efficiency in Refrigerated Vehicles to Prevent Food Spoilage

R. A. Pitarma ^a, J. E. Ramos ^b, N. Lima ^c, and M. G. Carvalho ^d

^a Polytechnic Institute of Guarda - ESTG, 6300-559 Guarda, Portugal, rpitarma@ipg.pt

^b Polytechnic Institute of Leiria - ESTG, Leiria, Portugal, jramos@estg.iplleiria.pt

^c University of Minho - CBE, 4710-057 Braga, Portugal, nelson@iec.uminho.pt

^d Technical University of Lisbon-IST, 1049-001 Lisboa, Portugal, maria@navier.ist.utl.pt

Abstract

An improper air distribution within refrigerated truck chambers is the major cause of inadequate road transport of perishable products under controlled temperature. Inadequate temperature control permits microbial and/or enzymatic deterioration. Experimental results in refrigerated long road vehicles show temperatures differences in the cargo of as much as 12°C. This paper presents a computational model to predict, and visualize, the temperature conditions (e.g. velocity, temperature and relative humidity) in refrigerated truck chambers. The model consists of a computer procedure, in which the general equations describing the airflow pattern and the heat/mass transfer in a refrigerated room are solved using the finite volume method. The effect of turbulence is described by the k-ε turbulence model. The computer model was experimental validated by measurements taken from a reduced-scale model designed to provide similarity with a prototype. The model was applied to calculate the indoor cold conditions provided by different types of air supply systems used in compartments of long road vehicles.

Key words: Computer simulation, refrigerated vehicles, air distribution, controlled temperature, food transport.

1 Introduction

The world-wide expansion of the frozen food industry and of the commercial exchange of perishables has given rise to the significant growth of road transport under controlled temperature, in order to preserve quality. The quality and nutritional value of food products stored in a cold state are affected by the time, temperature, air speed and relative humidity of the storage period. Inadequate temperature control permits microbial growth and/or enzymatic deterioration. Energy consumption is highly important. The reduction of energy should not be attained at the expense of quality of the product. Thus, the aim consists of reconciling these two (contradictory) factors.

In this context, an accurate understanding of indoor air motion is crucial to the design of chambers in providing cold conditions and increasing the energy efficiency of the mechanical and electrical systems. Economic values of the air circulation and its adequate distribution in the chamber are essential parameters. In accordance with the American Society of Heating, Refrigerating and Air-Conditioning Engineers, Inc. (ASHRAE) (1), an improper air circulation within refrigerated truck chambers is the major cause of inadequate road transport of perishable products under controlled temperature. Modifications in air-distribution systems can decrease the temperature spread and thus the necessary refrigeration power (6), and produce improvements in side wall temperatures (10). However, more research is required (3).

There are many potential configurations of air-distribution systems and a wide range of operating

conditions in refrigerated chambers, but few cases are used in practice. Experimental studies in this field are scarce. Such research is extremely expensive. An experimental full scale study of refrigerated long road vehicles was reported by (6). The study comprised comparative temperature measurements on three thin-wall and one conventional road refrigerated vehicle. The results reveal temperature differences in the cargo of a maximum of 12°C. Reduced-scale models have not previously been reported. In recent years, numerical simulation has made considerable progress in this research field. With the advanced computer simulation package Phoenix (Cham Ltd, UK), numerical calculations of velocity and temperature distributions in a 14 m³ refrigerated room were performed (11). The experimental validation was carried out only for temperature results showing reasonable agreement. Numerical predictions of refrigerated chambers with forced convection demonstrated that heat flow through the wall, air distribution and air circulation rate determined the temperature distribution in the chamber (8). The refrigerated room was a 11 m³ yogurt chamber and good agreement was obtained in experimental validation. A simplified modeling of a refrigerated vehicle compartment was proposed by (12). The results were satisfactory although only the airflow pattern was studied.

The current paper demonstrates a computational model to predict and visualize the road-transport conditions of perishable foods in refrigerated truck chambers. The model consists of a computer procedure, in which the general equations describing the airflow pattern and the heat/mass transfer in a refrigerated room are solved using the finite volume method. The effect of turbulence is described by the k-ε turbulence model.

2 Materials and methods

2.1 Governing equations

The time-averaged form of the governing equations for a steady, incompressible and turbulent flow may be represented in cartesian tensor notation by the general equation of the type:

$$\frac{\partial}{\partial x_i}(\rho U_i \phi) = \frac{\partial}{\partial x_i} \left(\Gamma_\phi \frac{\partial \phi}{\partial x_i} \right) + S_\phi \quad (1)$$

where: U_i is the mean velocity component (u, v, w) in the coordinate axis x_i (x, y, z); ϕ is the dependent variable; Γ_ϕ is the diffusion coefficient of the variable ϕ ; S_ϕ is a source term of the variable ϕ . In the equations for continuity, momentum (Navier-Stokes), thermal energy and concentration species, the variable ϕ acquires, respectively, the values 1, U_i (mean velocity in direction x_i), the specific enthalpy h and the mean concentration of water vapor w (specific humidity). For details see (8).

The turbulence is described by a transport equation for turbulent kinetic energy (k) and an equation for its rate of dissipation (ε), i.e. k - ε turbulence model (5). Thus, two additional transport equations with k and ε as the dependent variables need to be solved. The effects of buoyancy are included both on the equation of the vertical component of the velocity and in the turbulence model. The boundary conditions at the walls for velocity components, k-ε and thermal energy are specified using wall functions (5).

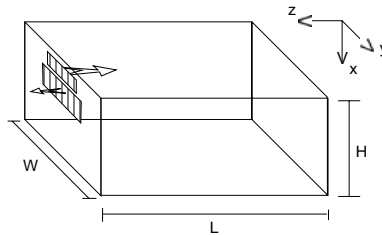
2.2 Numerical Solution Procedure

The conservative finite volume method was used for the discretization of the transport equations, employing a staggered grid for mean-velocity components relatively to scalar properties (7). The approximation of the convective fluxes applied at each control volume face was performed using the hybrid central/upwind difference scheme. One method based in the SIMPLE algorithm, was chosen for the pressure-velocity coupling correction (7). The solution of the discretization equations was obtained by a form of Gauss-Seidel line-by-line iteration.

2.3 Experimental Validation

To validate the computational model, experiments were conducted on a laboratory-scale. A physical modeling technique (8), based on dimensional analysis, was used to derive the physical properties from a

prototype truck chamber. The experimental enclosure consists of a $1.52 \times 0.72 \times 0.66 \text{ m}^3$ box with 6 mm Perspex glass walls (Figure 1). The apparatus is insulated with two tightly fitting layers of 50 mm thick expanded polystyrene. An auxiliary experimental installation which applies a computer linked air conditioning laboratory unit, was used to reproduce the inlet air flow conditions in the experimental chamber. The inlet air temperature, $T_o = 5.0^\circ\text{C}$, was controlled with a precision of 0.25°C . The air flows into the room, in the longitudinal direction, through a square supply opening placed near to the ceiling, and leaves the chamber through another lower square vent. The mean inlet velocity was $U_o = 3.1 \text{ m/s}$. However, velocity measurements were made to characterize the velocity distribution at the inlet section. The outside air temperatures was $T_e = 25^\circ\text{C}$. The internal room load (49.4 W) was produced, with an accuracy of 2 %, by electrically heated tapes laid over the floor area to produce a uniform load distribution.



H	W	L	Inlet		Outlet		m
			Height	Width	Height	Width	
0.66	0.72	1.52	0.06	0.24	0.12	0.32	

Fig.1 Diagram of the experimental reduced-scale model.

A vertical rake of 7 thermocouples (T type, $200 \mu\text{m}$ wire diameter) was used for temperature measurements. Temperature signals were acquired by a Data Translation A/D board (DT2811/DT756Y), connected to an HP Vectra personal computer, with a precision of 0.25°C . The sampling rate, selected after few preliminary runs, was 1Hz. (i.e. each one of the 7 channels was sampled every 7 s).

The air velocity magnitude $U = (u^2 + v^2 + w^2)^{0.5}$ measurements were obtained by a Dantec Streamline hot-wire anemometer system connected to an HP Vectra personal computer, with an omni-directional hot-film sensor (Low Velocity Transducer, Dantec 55R49). The control of the whole system, including acquired data and its treatment, was made by a Dantec StreamLine software support (10). The accuracy of measurements is less than $\pm 1 \% \pm 0.02 \text{ m/s}$.

2.4 Validation Results

The simulation model was used to predict the velocity and temperature fields in the reduced-scale model described above. The computations were performed using a $11 \times 18 \times 19$ control volumes grid. Because of the symmetry of the experimental chamber and their operating conditions, only half of the flowfield was covered by the computational domain. Grid-dependence tests were made which indicated that the differences between the results in this grid and a doubled grid ($22 \times 36 \times 38$) were not significant. The predictions were validated against experimental data acquired in the reduced model. Figure 2 illustrates an example of a comparison between computed and measured velocity and temperature non-dimensional profiles. The inlet conditions (U_o, T_o) were used to normalize the computational and measured results. The positive agreement obtained suggests that the model can be conveniently used in practice for engineering purposes.

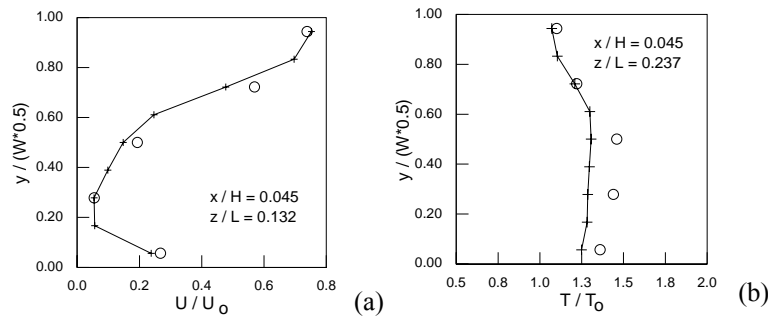
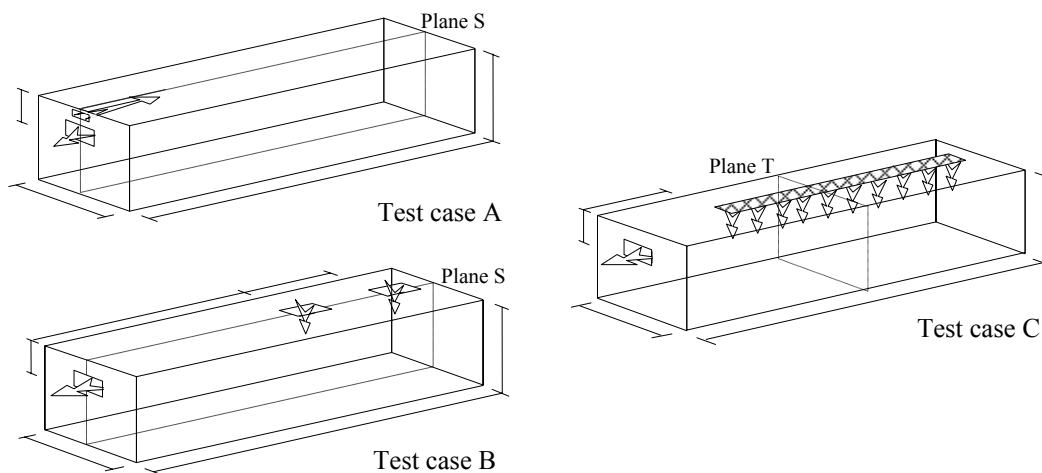


Fig.2 Predicted (+) and measured (o) non-dimensional velocity (a) and temperature (b) profiles.

2.5 Description of the cases considered

The considered cases are schematically represented in Figure 3. The simulated refrigerated truck chamber is a 12.25 x 2.20 x 2.10 m³ polyurethane-insulated room (100 mm thick). A detailed description of the body design and construction is available in (1,8). The geometrical parameters of the inlet and outlet sections are demonstrated in Table 1. The relevant functional parameters considered in the present simulation are presented in Table 2. The main goal of the three test cases (A, B and C) is to verify the performance of temperature quality achieved by the main ventilation systems. The test case C simulates a uniform air-supply system constituted by a duct in textile material. In all cases the same functional parameters were assumed, e.g. the rate of air circulation was assumed to be equal to 60 air changes per hour (10) (see Table 2). The internal thermal load from the floor was used to simulate the significant contributions of the respiration heat production of stored products. On the other hand, the heat gain through the floor was increased because of waste heat from the vehicle engine and from radiation from the road surface. So, the temperature of the external surface of the floor was assumed to be 10 °C above the ambient air temperature (1).



L	H	W	d _R	d _{B1}	d _{B2}	d _C
12.250	2.100	2.200	0.800	7.125	4.000	2.125 m

Fig.3 Diagram of the three different vehicle configurations studied (test cases).

Table 1. Geometric characteristics of the inlet and outlet sections of the air-distribution systems for each test case.

Parameters (units)		Test case		
		A	B	C
	Ceiling air duct	no	yes	yes
	Length (m)	-	0.25	9.95
Inlet section	Width (m)	1.00	1.00	0.40
	Height (m)	0.10	-	-
	Entire surface (m ²)	0.10	0.50	3.98
	Width (m)	1.20	1.20	1.20
Outlet section	Height (m)	0.30	0.30	0.30
	Entire surface (m ²)	0.36	0.36	0.36

Table 2. Main functional characteristics of the studied configurations.

Parameters (units)		Value
	Flow rate (m ³ /h)	3396.0
Supply air	Mean velocity (m/s)	9.50 (case A) 1.90 (case B) 0.24 (case C)
	Temperature (°C)	5.0
	Humidity (g/kg)/(%)	5.15/95
	Return air (outlet section) Mean velocity (m/s)	2.64
Thermal load (from floor)	Sensible/Latent heat (W/m ²)	19.0/58.0
Outside temperature	Air/Floor (°C)	37.0/47.0

2.6 Computational details

The computations were performed using a 21x22x50 control volumes grid. In accordance with the symmetry of chamber and operating conditions, only half of the geometry was covered by the computational domain. The iterative process was terminated after the normalized residuals have fallen below 0.09%. The computations were performed in a Hewlett Packard 9000 workstation, and the required time of CPU to achieve convergence was comprised between 4 h and 15 min of the test case C and 7 h and 26 min of the test case B.

3 RESULTS

Figure 4 provides examples of the predictions results for the temperature distribution obtained for the three test cases. In view of the considered problem (temperature control), only temperature fields are presented. In agreement with the flow-pattern characteristics, the planes that best illustrate the temperature distribution in the chamber for each test case are presented: plane S (symmetry plane) for the test cases A and B; plane T (transversal plane) for the test case C. In addition, Table 3 summarizes results of the temperature and relative humidity fields for the entire chamber, outlet section and region nearest

the floor. Maximum chamber temperatures were located near the lower front wall (test cases A and B) and at the bottom right along the side walls (test case C). The air-temperature spread of the vehicles was 2.4 - 4.1°C (Table 3). The predictions indicate that the maximum temperature (9.1°C) and maximum mean temperature (5.9°C) were reached in test case C. The configuration of test case B exhibited the most favorable mean temperature.

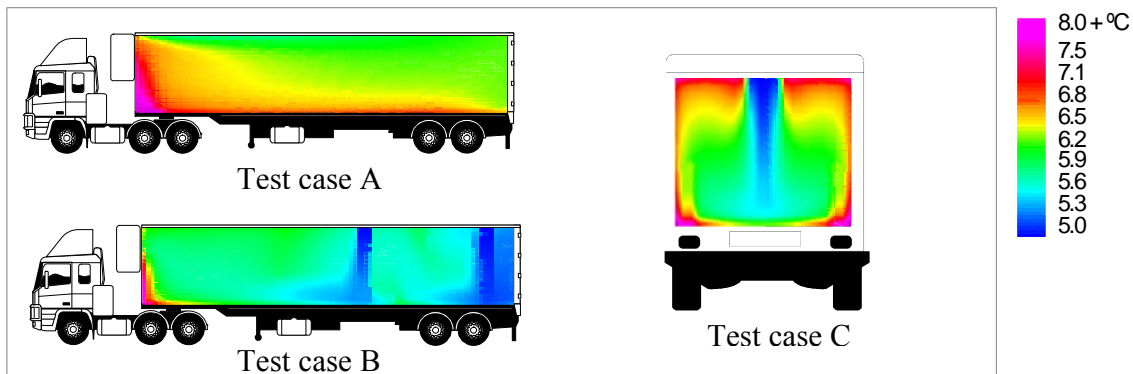


Fig.4 Predicted temperature distribution for the three test cases: A (symmetry plane: plane S); B (symmetry plane: plane S); C (transversal section: plane T).

Table 3. Summary of the predicted Temperature and Relative Humidity (average, maximum and spread) for the three test cases.

Parameters (units)	Test Case		
	A	B	C
$T_{av.}$ (°C)	5.8	5.7	5.9
$T_{max.}$ (°C)	7.4	8.4	9.1
$\Delta T_{(max.-min.)}$ (°C)	2.4	3.4	4.1
$RH_{av.}$ (%)	96.4	96.7	96.7
$\Delta RH_{(max.-min.)}$ (%)	5.9	7.3	5.9

4 DISCUSSION

In the most common method of air distribution (test case A), the air supplied into the chamber is carried out at high velocity (Table 2) with the purpose of instigating strong mixing, in order to reduce rapidly and as much as possible the gradients of temperatures. The cold-air distribution is relatively immune to disturbances and the mixing efficiency is a function of the inlet-jet velocity. However, the system often causes excessively high air velocities within the chamber and results in the high temperatures that occurs at the lower front of the chamber (Figure 4a) generated by the return convection current. This results in inadequate goods storage. In test case B, it was possible to reduce the inlet velocity by increasing of the inlet section area (Table 1), and decreasing short-circuiting air flow (Figure 4b). However, although the global mean temperature is similar, the results indicate higher gradients than for test case A (Table 3) due to the minor mixing effect. Another adequately placed air supply can probably help to solve the problem. In test case C, the low velocities (large inlet section) which characterize the whole storage zone can be decisive for the maintenance of specific goods. However, the high temperatures, particularly near the side walls (Figure 4c), suggest, the use of higher rate of air circulation than that used in the air-distribution systems of test cases. In conclusion, each air-supply method has its specific advantages and disadvantages which must be weighed against one another when selecting a method which is best suited for a given application. Finally, in spite of being considered well insulated vehicles (wall thickness ≈ 100 mm) with favorable operating parameters (e.g. airflow rate, thermal load, refrigeration power, operating temperatures) and no obstacles to air motion (empty chamber), the air-temperature spread of the vehicles was 2.4 - 4.1°C. Consequently, in more unfavorable cases the problem is much more serious. Moreover,

because of heat transfer phenomena the products-temperature spread will be higher still (higher than 7.9°C, (6,8)). More research in this field is recommended, since it represents an important problem for food protection.

5 CONCLUSION

A computational model for the simulation of three-dimensional non-isothermal flows in refrigerated truck chambers is presented. To validate the model, experiments have been conducted on a laboratory-scale in similarity conditions. Good agreement was found, indicating that the model can be reliably used in practice. The model was applied to calculate the indoor refrigeration conditions provided by the main types of air-supply systems used in compartments of long vehicles. The main conclusions are: The quality of the temperatures in refrigerated truck chambers is affected by the air-supply system; Temperature variations can be studied by the simulation model with versatility and low cost; A design for the cold-air distribution giving contributions to energy savings by decreasing the power needs and assuring temperature quality throughout the chamber is achieved; Finally, the model can be used by operators to decide when and how products must be loaded in order to preserve the quality and safety of perishables products.

6 REFERENCES

- American Society of Heating, Refrigerating and Air-Conditioning Engineers (ASHRAE). 1994. Handbook 1994 Refrigeration Systems and Applications. ASHRAE, Atlanta, USA.
- Awbi, H. B. 1995. Ventilation of buildings. Second Edition, E. & F.N. Spoon Press, London.
- Bennahmias, R. 1990. Transport de fruits et légumes frais à température dirigée. *Rev. Int. Froid*. 13:393-400.
- Jorgensen, F. E. 1994. A new concept for an automated hot-wire anemometer with fully integrated experiment manager. *Dantec Information*. 13: 2-9.
- Launder, B. E. and D. B. Spalding. 1984. The numerical computation of turbulent flows. *Compt. Methods Applied Mech. & Eng.* 3: 269-289.
- Nieuwenhuizen, G. H. and H. F. Meffert. 1986. Comparative experiments on three thin-wall and one conventional road vehicle. *Int. J. Refrig.* 9:303-309.
- Patankar, S. V. 1980. Numerical heat transfer & fluid flow, Hemisphere Publishing Corporation, Washington.
- Pitarma, R. A. 1998. Modelação matemática e experimental de câmaras frigoríficas de veículos. Ph.D. Thesis, Instituto Superior Técnico, Universidade Técnica de Lisboa, Lisboa, Portugal.
- Pitarma, R. A., J. E. Ramos and M. G. Carvalho. 2003. Computational and experimental reduced-scale modelling of air-conditioned rooms. *In proceedings of the Building Simulation 2003*. 3:1041-1045 Eindhoven, Holland.
- Scrine, G. R. 1986. Refrigerated vehicles - what next? *Int. J. Refrig.* 9:25-28.
- Wang H. and S. Touber. 1990. Distributed dynamic modelling of a refrigerated room. *Int. J. Refrig.* 13:214-222.
- Zertal-Ménia, N., J. Moureh and D. Flick. 2002. Modélisation simplifiée des coulements d'air dans un véhicule frigorifique. *Int. J. Refrig.* 25:660-672.